Vorinostat interferes with the signaling transduction pathway of T-cell receptor and synergizes with phosphoinositide-3 kinase inhibitors in cutaneous T-cell lymphoma

Magdalena B. Wozniak,[1] Raquel Villuendas,[1] James R. Bischoff,[2] Carmen Blanco Aparicio,[2] Juan F. Martínez Leal,[2] Paloma de La Cueva,[1] Mª Elena Rodriguez,[1] Beatriz Herreros,[1] Daniel Martin-Perez,[1] Maria I. Longo,[3] Marta Herrera,[4] Miguel Á. Piris,[1] and Pablo L Ortiz-Romero[4]

[1]Molecular Pathology Program, Spanish National Cancer Center, Madrid; [2]Experimental Therapuetics Program, National Cancer Center, Madrid; [3]Dermatology Department, Hospital Gregorio Marañon, Madrid, and [4]Dermatology Department, Hospital 12 de Octubre, Madrid, Spain

Acknowledgments: we are indebted to MC Marin for technical assistance, G Gómez for bioinformatics help, and to the Flow Cytometry Unit and the Tumor Bank Network which the collaborated in this work.

Funding: this work was supported by grants from the Ministerio de Ciencia y Tecnología (SAF2005-00221, SAF2008-03871), Comunidad Autónoma de Madrid (CAM 08.1/0011/2001.1), and Ministerio de Sanidad y Consumo (FISP05/1710, RETICS, PI051623, Acción Transversal del Cáncer, FIS PI080856) Spain. MBW is supported by FISP05/1710.

Manuscript received on July 6, 2009. Revised version arrived on September 15, 2009. Manuscript accepted on September 29, 2009.

Correspondence: Miguel A Piris, Spanish National Cancer Centre (CNIO), Melchor Fernández Almagro 3, Madrid 28029, Spain. E-mail: mapiris@cnio.es/ Pablo L Ortiz-Romero, Hospital 12 de Octubre, Av. De Cordoba s/n, Madrid 28041, Spain E-mail: portiz.hdoc@salud.madrid.org

The online version of this paper has a Supplementary Appendix.

ABSTRACT

Background

Vorinostat (suberoylanilide hydroxamic acid, SAHA), an inhibitor of class I and II histone deacetylases, has been approved for the treatment of cutaneous T-cell lymphoma. In spite of emerging information on the effect of vorinostat in many types of cancer, little is yet known about this drug's mechanism of action, which is essential for its proper use in combination therapy. We investigated alterations in gene expression profile over time in cutaneous T-cell lymphoma cells treated with vorinostat. Subsequently, we evaluated inhibitors of PI3K, PIM and HSP90 as potential combination agents in the treatment of cutaneous T-cell lymphoma.

Design and Methods

The genes significantly up- or down-regulated by vorinostat over different time periods (2-fold change, false discovery rate corrected *P* value<0.05) were selected using the short-time series expression miner. Cell viability was assessed *in vitro* in cutaneous T-cell lymphoma cells through measuring intracellular ATP content. Drug interactions were analyzed by the combination index method with CalcuSyn software.

Results

The functional analysis suggests that vorinostat modifies signaling of T-cell receptor, MAPK, and JAK-STAT pathways. The phosphorylation studies of ZAP70 (Tyr319, Tyr493) and its downstream target AKT (Ser473) revealed that vorinostat inhibits phosphorylation of these kinases. With regards to effects on cutaneous T-cell lymphoma cells, combining vorinostat with PI3K inhibitors resulted in synergy while cytotoxic antagonism was observed when vorinostat was combined with HSP90 inhibitor.

Conclusions

These results demonstrate the potential targets of vorinostat, underlining the importance of T-cell receptor signaling inhibition following vorinostat treatment. Additionally, we showed that combination therapies involving histone deacetylase inhibitors and inhibitors of PI3K are potentially efficacious for the treatment of cutaneous T-cell lymphoma.

Key words: vorinostat, gene expression, cutaneous T-cell lymphoma, synergy, HDAC inhibitors.

Citation: Wozniak MB, Villuendas R, Bischoff JR, Aparicio CB, Martínez Leal JF, de La Cueva P, Rodriguez ME, Herreros B, Martin-Perez D, Longo MI, Herrera M, Piris MÁ, and Ortiz-Romero PL. Vorinostat interferes with the signaling transduction pathway of T-cell receptor and synergizes with phosphoinositide-3 kinase inhibitors in cutaneous T-cell lymphoma. Haematologica. 2010;95:613-621. doi:10.3324/haematol.2009.013870

Introduction

Cutaneous T-cell lymphomas (CTCL) are a heterogeneous group of extranodal non-Hodgkin's lymphomas that are characterized by an initial accumulation of malignant T cells in the skin.[1] Mycosis fungoides and Sézary syndrome are the most frequently encountered forms of CTCL. The survival and treatment of patients with mycosis fungoides or Sézary syndrome depends mainly on the stage of the disease at diagnosis. However, at present no curative treatment for CTCL is available, and the aim of therapy is to maintain a long-term complete remission and preserve quality of life.

In a previous study we identified a set of genes and pathways associated with resistance to psoralen plus ultraviolet A (PUVA) radiation with or without interferon-α therapy in patients with mycosis fungoides.[2] Using Connectivity Map,[3] which combines the resistance gene expression signature with a database of expression profiles of bioactive small molecules, we identified several molecules as agents potentially able to reverse resistance to PUVA with or without interferon-α therapy. These molecules included a protein kinase C (PKC) inhibitor, H-7; heat shock protein 90 (HSP90) inhibitors, geldanamycin and tanespimycin (17-allylamino-geldanamycin 17-AAG); histone deacetylase (HDAC) inhibitors, vorinostat and scriptaid; a cyclin-dependent kinase 2 (CDK2) inhibitor, GW-8510; cyclosporines and anti-bacterial and anti-protozoal agents (*Online Supplementary Table S1*).

HDAC inhibitors are relatively new anti-cancer drugs showing efficacy in a wide range of both hematologic and solid cancers.[4,5] Vorinostat (suberoylanilide hydroxamic acid - SAHA, Zolinza™) is a pan-HDAC inhibitor which inhibits the enzymatic activity of histone deacetylases resulting in the accumulation of acetylated histones and non-histone proteins. Vorinostat causes caspase-dependent apoptotic cell death, caspase-independent autophagic cell death and cell cycle arrest of a wide variety of transformed cells.[6] Modulated expression of 2-10% of genes in malignant cells has been described.[7,8] *CDKN1A* (*P21, WAF1/CIP1*) is a gene commonly induced following vorinostat treatment and could be related to the arrest in G1 phase of the cell cycle,[8] while the cyclin D1, *ERBB2* and thymidylate synthase genes are among those repressed following vorinostat treatment.[9] Other targets of vorinostat include transcription factors (MyoD, E2F-1, Smad 7, TF11E and GATA1), tumor suppressors (p53, Rb), chaperone protein (Hsp90) as well as factors involved in cell motility (α-tubulin), apoptosis (Bcl-2 family), angiogenesis (HIF-1α) and reactive oxygen species (thioredoxin).[6-8,10] Such a multiplicity of targets could partly explain the efficacy of vorinostat as an anticancer agent. However, the exact mechanism, the kinetics of gene expression and players involved in resistance to this drug are still unknown.

Clinical trials in patients with refractory CTCL demonstrated an objective overall response of 30%[11] following vorinostat treatment. Subsequently, vorinostat was approved by the USA Food and Drug Administration for the treatment of CTCL. Presently, vorinostat is being investigated in clinical trials both as monotherapy and in combination with various anticancer drugs. Vorinostat has been reported to have synergistic or additive effects when used with several anticancer agents, including anthracyclines, fludarabine, flavopiridol, imatinib, bortezomib, isotretinoin, antiangiogenic agents and TNFS10.[12] At the time of writing, there are 137 registered clinical trials involving this drug (*www.cancer.gov*). In 41 trials vorinostat is used as a monotherapy, while in as many as 96 clinical trials, vorinostat is used in combination with other therapies. The shift from monotherapy to combination therapy in clinical trials is heralding future applications of specific HDAC inhibitors. However, in order to exploit combination drug therapies fully, precise information is needed on the mechanism of action of the drugs and on the times at which expression of particular genes is altered.

Stimulation of the T-cell antigen receptor (TCR) induces activation of multiple protein tyrosine kinases, resulting in phosphorylation of multiple intracellular substrates, including TCRξ and CD3 chains, zeta chain associated protein 70 (ZAP70), and phospholipase C-γ1.[13] These early biochemical events are an obligatory step in TCR signal transduction. CTCL cells show a considerable degree of T-cell activation, as characterized by the increased expression of HLA-DR, interleukin-2 receptor-α (CD25) and transferrin receptor.[14] Activated malignant T cells have the ability to switch on the production of signaling molecules and cytokines. Hence, the progression of mycosis fungoides is accompanied by a shift in cytokine profile from Th1 to Th2.[15]

In this study, we investigated the alterations in gene expression profile, acetylation, proliferation and cell death over time in five CTCL cell lines after vorinostat treatment. Additionally, in this preclinical study we evaluated the combined effect of vorinostat with phosphoinositide 3 kinase (PI3K), PIM and HSP90 inhibitors in CTCL.

Design and Methods

Tissue culture and reagents

Human CTCL cell lines and culture conditions are described in the *Online Supplementary Design and Methods*. Vorinostat was provided by Merck (Boston, Massachusetts), LY294002 was purchased from Calbiochem (La Jolla, CA, USA) and 17-AAG was obtained from Sigma (St Louis, MO, USA). ETP-45628 and ETP-39010 were developed by the Experimental Therapeutics Program at CNIO (Madrid, Spain).

Viability, apoptosis, and cell cycle

Cell viability was measured using a CellTiter-Glo luminescent cell viability assay (Promega, Madison, WI, USA) following the manufacturer's instructions. The flow cytometry analysis of cell cycle and apoptosis are described in the *Online Supplementary Design and Methods*.

Western blotting

Histone acetylation and phospohorylation were studied by western blotting, as described more extensively in the *Online Supplementary Design and Methods*.

Oligonucleotide microarray analysis of gene expression

The transcriptional profile of vorinostat was characterized by oligonucleotide microarray analysis of CTCL cells treated with vorinostat (5 μM for 0–24 h), using the human Agilent microarray (Agilent Technologies, Inc., Santa Clara, CA, USA). Total RNA extraction and purification, amplification, labeling, hybridization to Agilent 44K Human Whole Genome microarrays and scanning of image output files were performed according to the manufacturer's instructions. The data were normalized with the use of Feature Extraction (v.9.0)

Table 1. Sensitivity to vorinostat, ETP-45628, LY294002, ETP-39010, and 17-AAG for a panel of CTCL cell lines from the proliferation/viability assays (CellTiter-Glo Viability Assay). Proliferation/viability was analyzed after 3 days of treatment unless stated otherwise.

Cell lines	IC_{50} [μM]					
Name	Vorinostat	ETP-45628	LY294002	ETP-39010*	ETP-39010	17-AAG
HH	0.146	0.442	1.797	17.051	5.042	0.803
HuT78	2.062	1.444	10.853	5.977	2.695	0.235
MJ	2.697	0.603	10.158	3.083	1.286	0.644
MYLA	1.375	1.033	28.776	4.639	2.708	0.146
SeAx	1.510	1.500	34.669	4.194	3.190	0.258

** Proliferation/viability was analyzed after 48 hours.*

software.

Assignment of genes to temporal expression profiles was conducted using the Short Time Series Expression Miner (STEM).[16] The significant genes were annotated and classified using FatiGO+[17] and Ingenuity Pathway Analysis software v.6.3 (Ingenuity Systems, Inc., Redwood City, CA, USA). Molecules (drugs) that could reverse the gene expression signatures associated with poor prognosis and drug resistance were identified using Connectivity Map.[3]

Statistical analysis

Group comparisons of parametric data were performed using Student's t-test. Statistical analyses were carried out with the SPSS software package, version 13.0. The mean inhibitory concentration 50% (IC_{50}) of drugs was calculated using GraphPad Prism software. The combination index (CI) method described by Chou and Talalay (CalcuSyn software, Biosoft) was used to determine whether the effect of drug combinations were synergistic, additive, or antagonistic. Synergy, additivity, and antagonism were defined by a CI less than one, a CI of one and a CI greater than one, respectively.

Further details of the experimental procedures and statistical analysis are provided in the *Online Supplementary Design and Methods*.

Results

Vorinostat induces cell death, cell cycle arrest and accumulation of acetylated histones in cutaneous T-cell lymphoma cells

The inhibitory effect of vorinostat on the viability of CTCL cell lines was examined through a CellTiter-Glo assay using various concentrations of vorinostat (0.01, 0.05, 0.15, 0.5, 1.25, 4, 10, 35, and 100 μM) for 72 h. All CTCL cell lines were sensitive to the investigated HDAC inhibitor. The inhibitory effect of vorinostat was reflected as a dose-dependent reduction in cell proliferation/viability. The IC_{50} of proliferation was determined at 0.146 μM in HH cells, at 2.062 μM in HuT78 cells, at 2.697 μM in MJ cells, at 1.375 μM in MylA and at 1.510 μM in SeAx cells (Table 1).

In addition, we investigated whether the observed sensitization effect was related to the increase in apoptosis. To study this aspect of vorinostat treatment, HH, HuT78, MJ, Myla and SeAx cells were treated with various doses of vorinostat. Apoptosis was detected after 24 – 48 h through annexin V and propidium iodide staining. Time- and dose-dependent increases in the populations of apoptotic cells were observed in all the cell lines (*Online Supplementary Figure S1A*). HH cells were most responsive to vorinostat, with the percentage apoptosis being 18±3.9% already after 24 h and 44±1.6% after 48 h. HuT78 cells were less sensitive to vorinostat with percentage apoptotic death being 3.4±1.3% and 17±3.9% at 24 h and 48 h, respectively. The percentage death among MJ, Myla and SeAx cell lines was approximately 26% after 48 h.

We also investigated the effect of vorinostat on cell cycle progression in CTCL cell lines by treating the cells with vorinostat or vehicle alone (dimethylsulfoxide, DMSO) for 24 h and 48 h and analyzing the cell cycle distribution by flow cytometry. The percentage of cells in the S phase decreased in MJ and SeAx cells compared with that in control cells. G2/M cell cycle arrest was induced in HuT78 cells, while a G0/G1 phase arrest was detected in Myla, MJ and SeAx cells (*Online Supplementary Figure S1B*).

The effect of vorinostat on histone acetylation status in human CTCL cell lines was determined by western blot analysis. CTCL cells were exposed to 5 μM of vorinostat for 0, 0.5, 1, 2, 4, 8, 12 and 24 h. As shown in *Online Supplementary Figure S2*, all four core nucleosomal histones (H2A, H2B, H3, and H4) become hyperacetylated following culture in the presence of vorinostat when compared to culture with the DMSO control. These effects were visible after exposure of 0.5 h (Myla) and showed a time-dependent increase.

Transcriptional profile following vorinostat treatment

Based on flow cytometry data, the CTCL cells were cultured in the presence of vorinostat for 24 h. Gene expression data were obtained from two independent microarray hybridizations at various time points. Data were then analyzed using STEM and genes that were significantly up- or down-regulated (false discovery rate, FDR<0.05) were analyzed further. The number of genes altered increased progressively during the 24 h of treatment (Figure 1A-B). Around 20% of genes on the array were significantly activated or repressed in response to vorinostat. The number of genes that were modulated in response to treatment increased from 318 (HH), 424 (HuT78), 528 (MJ), 301 (Myla) and 155 (SeAx) at 4 h to 3512 (HH), 2379 (HuT78), 3081 (MJ), 2022 (Myla) and 3275 (SeAx) at 24 h.

The functional analysis of genes that were up- or down-regulated in response to vorinostat treatment revealed pathways that have previously been identified as being altered by the drug, including cell proliferation, apoptosis and cell cycle, as well as new pathways that have not been reported previously but could contribute crucially to the understanding of the mechanism of action of this HDAC inhibitor (*Online Supplementary Table S2*).

Consistent with previous findings by Ruefli *et al.*[18] vorinostat modulated expression of key apoptosis genes,

such as *IRAK1*, *FAS*, *CASP6*, *BID*, *BIRC4*, *cFLAR*, *CAPN2*, *BCL2L1*, *TNFRSF1A* and *TNFRSF10A*. Multiple mitogen-activated protein kinase (MAPK) signaling pathway members were also altered by vorinostat. Interestingly, the expression of genes involved in signal transduction and response to stress (*MAPK12*, *MAP3K6*, *MAPK13*, *MAP4K1*) was inhibited, while genes playing a role in the induction of apoptosis (*MAPK1*, *MAPK8*, *MAPK9*, *MAPK10*, *MAPK14* *MAP2K6*, *MAP3K7*, *MAP3K10*, *MAP4K2*, *MAP2K2*) were up-regulated.

HDAC inhibition of CTCL cells modulates the expression of genes involved in cell cycle.[7,19] Thus, vorinostat down-regulated genes required for G1/S transition (often aberrantly expressed in tumor cells), including *E2F1*, *E2F4*, *E2F5*, *SKP2*, *CDC25A*, *CDK4*, *CDK6*, *CDC6*, *CDC25B* and several cyclins (cyclins *A2*, *D2*, *D3*, *E2*), as well as G2/M phase regulators (*CDC23*, *CDC25B*, *CHEK1*). Furthermore, vorinostat treatment induced expression of genes with antiproliferative or arrest functions (*CDKN2A*, *CDKN2B*, *CDKN2C*, *CDKN2D*, *CDKN1A*, *CDKN1C*) (*Online Supplementary Figure S3*).

Additionally, significant changes after vorinostat treatment were observed in members of the JAK/STAT pathway, cytokine-cytokine receptor interactions and expression of the members of tumor necrosis factor (TNF) receptor superfamily. Vorinostat also produced significant alterations in the network of interleukins (IL) and their receptors; it inhibited expression of *IL4*, *IL5*, *IL10*, *IL11*, *IL13*, *IL15A*, *IL19*, *IL21*, *IL29*, *IL2RB*, *IL4R*, *IL6R*, *IL10RA*, *IL15RA*; and enhanced expression of *IL1A*, *IL6*, *IL9*, *IL12A*, *IL15*, *IL22*, *IL23A*, *IL24*, *IL1RAP*, *IL3RA*. Interestingly, many of the repressed interleukins are known to enhance cell growth, proliferation and promote Th2 responses, which are a hallmark of CTCL pathogenesis. Furthermore, we found that the expression profile of a set of chemokines and their receptors was also shifted by vorinostat treatment. The down-regulated set included genes related to T-cell migration and chemotaxis, such as *CCL1*, *CCL22*, *CCL26*, *CCL28*, *CXCL10*, *CXCL13*, *CXCL16*, *CCRA*, *CCR4*, *CCR6*, *CXCR3* and *CXCR4*, whereas the genes

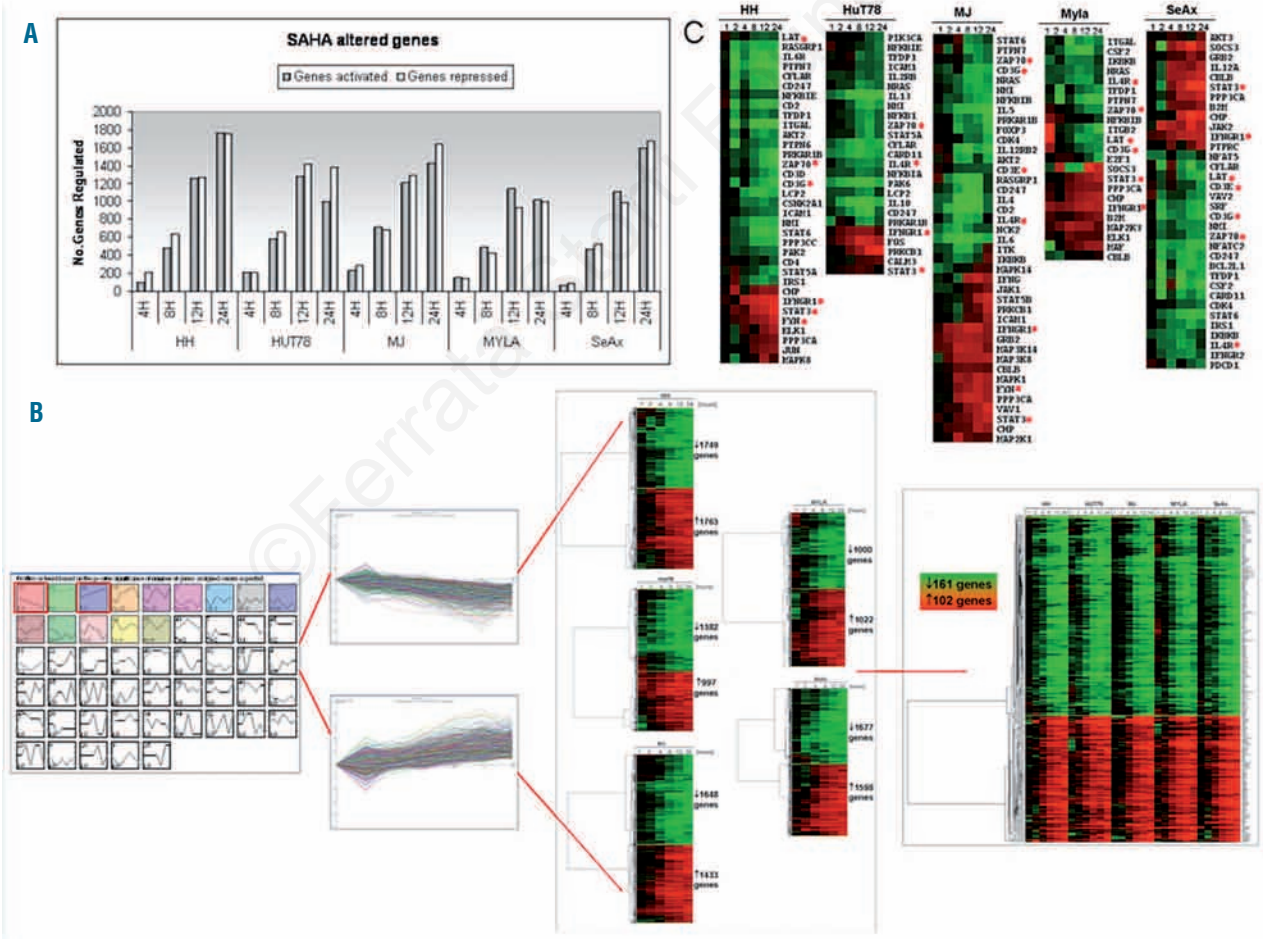

Figure 1. Gene expression profiles of vorinostat (SAHA)-regulated genes. (**A**) Numbers of genes up- and down-regulated at each time point after treatment with vorinostat. Number of genes with significant profile that were differentially expressed by at least 2-fold from time 0 h to at least one later time point in response to vorinostat are shown. (**B**) Short time series expression miner (STEM) analysis flowchart. The figure represents selected up- and down-regulated profiles and significant genes within selected profiles are visualized for each cell line. Genes selected as differentially expressed were clustered using CLUSTER and visualized by TreeView. Genes were hierarchically clustered based on standard correlation coefficients. (**C**) Functional clustering of vorinostat-regulated T-cell receptor associated genes. The red asterisks indicate genes chosen for quantitative RT-PCR validation.

induced by vorinostat included *CCL19*, *CCL20*, *CCL27*, *CXCL9*, *CXCL11*, *CX3CL1*, *CCR2* and *CCR6*. We also observed alterations in the expression of the remaining members of the JAK/STAT pathway, with suppression of *STAT6*, *STAT5A*, *SOCS2*, *SOCS6* and *SOS* accompanied by enhanced expression of *STAT1*, *STAT2*, *STAT3*, *STAT5B*, *SOCS3*, *IFNAR2*, *INFG*, *IFNGR1* and *JAK1*.

The repressive influence of vorinostat on TCR pathway signaling was common to all the CTCL cell lines. Thus, vorinostat repressed a remarkably large set of genes directly associated with the TCR, together with molecules acting downstream, including *ZAP70*, *LAT*, *VAV2*, *CD247*, *CD3D*, *CD3E*, *CD3G*, *CD4*, *IL4*, *IL5*, *IL10*, *IL13*, *IL4R*, *IL6R*, *PTPN6*, *PAK2*, *PAK6*, *ICAM1*, *NMI*, *FOXP3*, while upregulated genes included *FYN*, *IFNG*, *IFNGR1*, *IL12A* and others (Figure 1C). TCR signaling has been found to be associated with resistance to PUVA with or without interferon-α therapy,[2] which could explain why vorinostat sensitizes patients resistant to this therapy.

Validation of expression profiles of selected genes by quantitative real-time polymerase chain reaction

To verify changes in gene expression detected by our microarray analysis, we performed quantitative real-time polymerase chain reaction (PCR) analysis on eight genes belonging to the TCR pathway, whose expression profiles were altered by vorinostat in at least two cell lines. These genes were *ZAP70*, *STAT3*, *FYN*, *IFNGR1*, *CD3G*, *LAT*, *IL4R* and *CD3E*. As shown in *Online Supplementary Figure S4A-H* there was a strong correlation between the microarray and real-time PCR data for all eight genes.

Vorinostat decreases T-cell receptor activation through inhibition of kinase phosphorylation

Considering the critical role of ZAP70 in transmitting signals from the TCR signaling complex, we examined the ability of vorinostat to inhibit tyrosine phosphorylation in two of the CTCL cell lines. Cells from two representative cell lines, HuT78 (Sézary syndrome) and Myla (mycosis fungoides), were treated with vorinostat for 0.5, 1, 6 and 24 h at the concentrations of 5 and 25 μM. Phosphorylation of Tyr319 and Tyr493 within the activation loop results in enzymatic activation of ZAP70.[20] A decrease in phosphorylation of ZAP70 at Tyr493 after vorinostat treatment was observed in HuT78 cells after 0.5 h (25 μM vorinostat) and 1 h (5 μM vorinostat) and in Myla cells after 1 h for both concentrations. Phosphorylation of Tyr319 was diminished after 1 h (25 μM) and 6 h (5 μM) in HuT78 cells and after 1 h (25 μM) in Myla cells (Figure 2A). In both cases the inhibition of tyrosine phosphorylation was time- and concentration-dependent. Meanwhile, vorinostat modestly decreased total cellular level of ZAP70.

Tyrosine phosphorylation of ZAP70 correlates well with its increased kinase activity and downstream signaling events. To extend our understanding of the potential impact of vorinostat on T-cell signaling we evaluated the downstream effector molecules. The PI3K/AKT pathway has been shown to be implicated in signal transmission leading to the activation, differentiation and survival of T-lymphocytes.[21] In HuT78 cells the activating phosphorylation of AKT within the carboxy terminus at Ser473 was decreased already after 0.5 h of exposure to 25 μM of vorinostat and was further reduced at 1, 6 and 24 h. In the Myla cell line a slight reduction in AKT (Ser473) phosphorylation was observed after exposure to vorinostat for 1 h, followed by a significant reduction after 24 h. Vorinostat also decreased the total AKT levels in a dose-dependent manner (Figure 2B).

Combinations of vorinostat with phosphoinositide 3 kinase, PIM and heat shock protein 90 inhibitors

Vorinostat, being a multi-HDAC inhibitor, could be suitable for use in combination therapy with other anti-neoplastic agents. As candidates for combination therapy we selected PI3K inhibitors (LY294002, ETP-45658), a PIM kinase family inhibitor (ETP-39010) and a HSP90 inhibitor (17-AAG). These inhibitors were chosen following an analysis of the genes targeted by vorinostat or Connectivity Map data. GSK-3β (a PI3K substrate) and PIM1/PIM2 were up-regulated after vorinostat treatment (Figure 3A). HSP90 (a target of 17-AAG) was down-regulated, but was included in this analysis since it had the best score in the Connectivity Map analysis.

The sensitivity of CTCL cells to exposure for 72 h to each of the compounds individually or in combination was determined by a Luminescent Cell Viability Assay. The IC_{50} values for LY294002 ranged between 1.797 μM (HH cells) and 34.669 μM (SeAx cells). The IC_{50} values for a more potent and selective PI3K inhibitor, ETP-45658,[22] ranged from 0.442 μM (HH cells) to 1.5 μM (SeAx cells), being 4-28 times lower than those for LY294002. We also tested the inhibitor of PIM kinase family, ETP-39010, which showed IC_{50} values varying from 1.286 μM (MJ cells) to 5.042 μM (HH cells) after 72 h of exposure and from 3.083 μM (MJ cells) to 17.051 μM (HH cells) after 48 h of exposure. The IC_{50} values for the HSP90 inhibitor 17-AAG were in the nanomolar range for all the cell lines, with Myla cells being the most sensitive (146 nM) and HH cells the least sensitive, as shown by the highest IC_{50} value of 803 nM (Table 1).

To study possible synergy between vorinostat and other drugs, approximately equipotent concentrations of each drug were used. Values of the combination index (CI) were calculated using CalcuSyn software with a formula initially proposed by Chou and Talalay. The drugs were used in constant ratios to determine the effectiveness of the combinations. When at least 80% of CI values for a combination in all cell lines were less than one, the drug combination was considered to be synergistic. Similarly, if more than 80% of the CI values were higher than one the drug was considered antagonistic. Otherwise, the drug was considered to have an additive effect with a synergistic or antagonistic tendency.

Combined treatment of vorinostat with LY294002 demonstrated moderate to strong synergy, usually with the best CI values for IC_{50} concentrations and above for all CTCL cell lines, with synergy being strongest in the SeAx cell line. Co-administration of vorinostat with the more potent and selective PI3K inhibitor ETP-45658 also showed clear synergism at the concentration of 0.5 times the IC_{50} and above (Figure 3B). Concomitant as well as sequential addition (addition of the drug after 24 h pretreatment with vorinostat) of a PIM inhibitor (ETP-39010) resulted in additive to synergistic effects in HuT78 and SeAx Sézary syndrome cell lines, an additive to antagonistic effect in Myla cells and varying results in HH and MJ cell lines (Figure 3C). Clear antagonism was observed when vorinostat was concomitantly administered with 17-AAG, an inhibitor of HSP90 (Figure 3D). The results of combination therapy seemed to be conversely related to the expression changes

of the targets of inhibitors used following treatment with vorinostat. In summary, a synergistic/additive effect of combination therapy was demonstrated for the compounds targeting genes whose expression was up-regulated by vorinostat.

Discussion

Recent reports have highlighted the pre-clinical activity of HDAC inhibitors in human leukemia and lymphoma cells, as well as the promising results of vorinostat in a substantial proportion of patients with advanced CTCL (response rate of around 30%),[11] leading to the approval of this drug by the USA Food and Drug Administration. The focus on the therapeutic use of vorinostat is currently its application in combination therapies, reflected by numerous ongoing clinical trials. However, the mechanism of action of vorinostat, essential for efficient use of the drug alone or in combination, has not been fully clarified. A likely model for the anti-tumor action of vorinostat is inhibition of HDAC activity and subsequent accumulation of acetylated nucleosomal histones, leading to the alteration of genes involved in the regulation of differentiation, apoptosis and tumor growth.[23] The present study showed that vorinostat, at the concentration of 5 μM, induces apoptosis of CTCL cells through several different but non-exclusive mechanisms.

In CTCL the balance between cell proliferation and cell death is altered, contributing to a clonal expansion of cancer cells. Zhang *et al.*[24] investigated the expression of apoptosis regulators in CTCL cells reporting a shift of the equilibrium between inducers and inhibitors in favor of the apoptosis inhibitors. BCL2L1 (BCL-xL), MCL1, BAD and BAX, but not BCL-x, were found to be expressed in CTCL and could be sufficient for survival of malignant CTCL cells. Like Rosato *et al.*,[25] we observed decreases in the expression of BCL2L1, MCL1, BCL2, BID which may be related to the enhanced sensitivity to apoptosis occurring after treatment with vorinostat. Moreover, our data revealed alterations in both the intrinsic pathway of apoptosis (CASP9, CASP7, APAF1) and the extrinsic pathway (FAS, BID, cFLAR) following treatment with vorinostat. As previously observed in leukemic cells,[7,18] we noted activation of the intrinsic apoptotic pathway through up-regulation of CASP9 and a key downstream effector of the pathway - APAF1. Furthermore, we identified decreases in the expression of important members of the extrinsic apoptosis pathway, such as FAS, BID, and cFLAR (CASP8), following treatment with vorinostat. The extrinsic apoptotic pathway, either alone or together with the intrinsic pathway, has been previously described to be altered upon

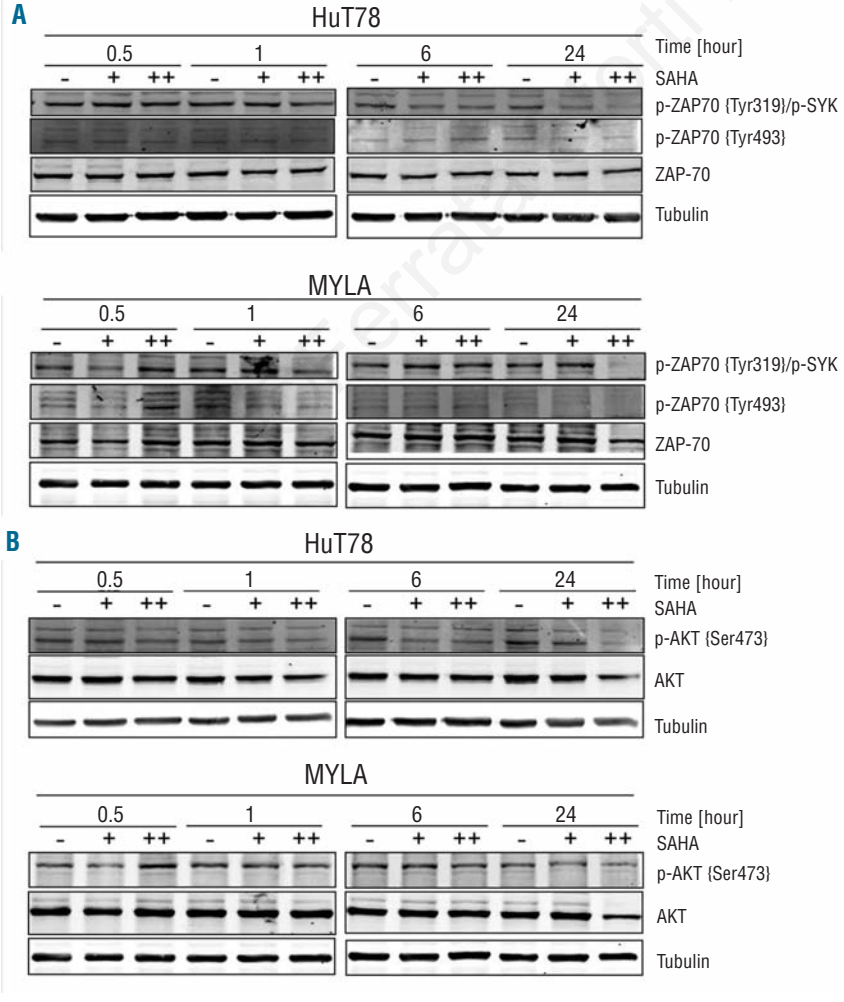

Figure 2. Effect of vorinostat (SAHA) on TCR-related genes. HuT78 and Myla cells were incubated with 5 μM (+) or 25 μM (++) of vorinostat for 0.5, 1, 6 and 24 h. Whole cell lysates were examined by western blotting for phospho-ZAP70 (Tyr319 and Tyr493) (A) and phospho-AKT (Ser473) (B). Total ZAP-70 and AKT were used as controls, respectively. Tubulin was used as a loading control of total proteins.

treatment with HDAC inhibitors in other types of cancer, including leukemias,[25] and head and neck malignancies.[26] As vorinostat promotes up-regulation and activation of multiple pro-apoptotic factors we believe that down-regulation of FAS, BID and cFLAR could be a compensatory mechanism of CTCL cells in response to treatment. Additionally, vorinostat inhibited members of the TNF receptor superfamily and their downstream signaling cascades, expressed in activated T cells, which are responsible for the transduction of survival and proliferation signals, while up-regulated genes mediated signals for apoptosis. Consistent with the previous findings of Duvic *et al.*[11] and Fantin *et al.*[27] we observed modulation of the JAK/STAT pathway, including suppression of *STAT6*, *STAT5A*, *SOCS2*, *SOCS6* and *SOS* accompanied by enhanced expression of *STAT1*, *STAT2*, *STAT3*, *STAT5B*, *SOCS3*, *IFNAR2*, *INFG*, *IFNGR1* and *JAK1*.

Finally, vorinostat repressed several members of the TCR signaling pathway as well as factors acting downstream. Vorinostat treatment caused down-regulation of *ZAP70*, *LAT*, *VAV2*, *CD247*, *CD3D*, *CD3E*, *CD3G*, *CD4*, *IL4*, *IL5*, *IL10*, *IL13*, *IL4R*, *IL6R*, *PTPN6*, *PAK2*, *PAK6*, *ICAM1*, *NMI*, and *FOXP3* while it up-regulated *FYN*, *IFNG*, *IFNGR1*, and *IL12A* suggesting a shift in the balance of T helper cells from Th2 (the phenotype of malignant T cells) to Th1. In our previous study we related the TCR pathway to resistance to treatment with PUVA with or without interferon-α.[2] To our knowledge, this is the first report that identifies the TCR signaling pathway as a target for vorinostat.

T-lymphocytes play a crucial role in the immune response, both as direct effector cells and as regulatory cells that modulate the functions of other cell types. One of the earliest recognizable events after TCR stimulation is activation of LCK (p56lck) and FYN (p59fyn), which results in phosphorylation of tyrosine residues. Subsequently, ZAP70 tyrosine kinase is recruited to the TCR where it is activated by LCK through tyrosine phosphorylation. ZAP70 is a key signaling molecule in T cells, where it couples the antigen-activated TCR to downstream signaling pathways.[28] Once ZAP70 has been activated, LCK and ZAP70 presumably act synergistically to phosphorylate specific downstream substrates, which in turn orchestrate the cytoplasmic signaling cascades leading to T-cell activation. These central roles of LCK and ZAP70 in TCR signal-

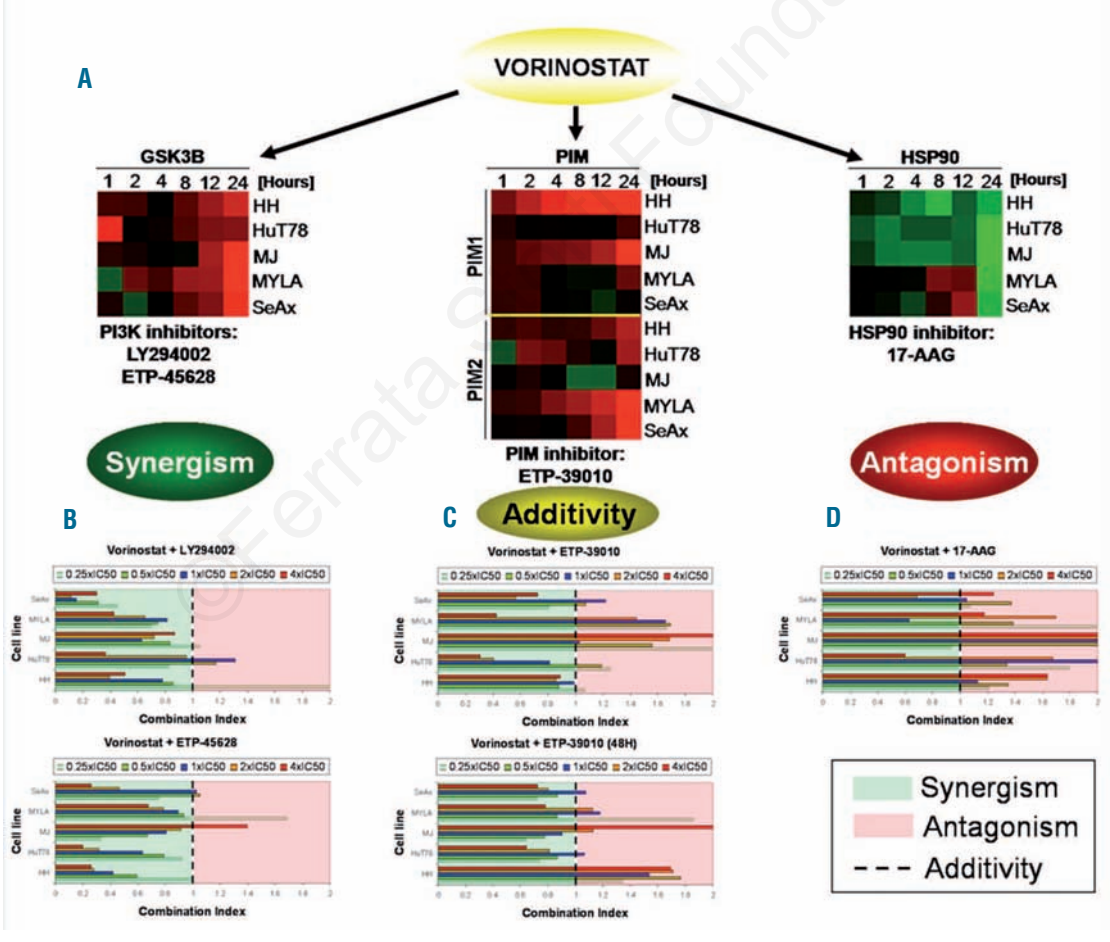

Figure 3. Combination studies of vorinostat with PI3K, PIM and HSP90 inhibitors in cutaneous T-cell lymphoma (CTCL) cells. (A) Effect of vorinostat on the targets of the inhibitors used for combination studies: PI3K inhibitors (GSK-3β - left panel), PIM inhibitor (PIM1 and PIM2 – middle panel) and HSP90 inhibitor (17-AAG – right panel) in five CTCL cell lines. The HH, HuT78, MJ, MYLA, and SeAx cells were treated with 5 μM of vorinostat over 24 h. The gene expression values were normalized with respect to time 0. The selected genes were visualized using CLUSTER and TreeView. (B) Synergistic interactions between vorinostat and PI3K inhibitors (LY294002 and ETP-45658). (C) Additive interactions for concomitant and sequential co-administration of vorinostat with PIM inhibitor (ETP-39010). (D) Antagonistic interactions between vorinostat and HSP90 inhibitor (17-AAG). (B, C, D) Synergistic, additive, or antagonistic effects of the drug combinations were determined by calculating the combination index value (CI) by isobologram analysis with CalcuSyn software. A CI = 1 indicates synergism, CI ± 1 indicates additivity and CI > 1 indicates antagonism.

ing have been amply documented. ZAP70 causes phosphorylation of LAT (linker for activation of T-cells), which in turn activates important downstream signaling pathways, including PKC, PKB, and MAPK, such as extracellular signal-regulated kinase (ERK), p38 MAPK, and c-JUN N-terminal kinase (JNK).[29] The PI3K/AKT pathway is also necessary for the survival of T-lymphocytes through both increased expression of BCL-XL and as a consequence of the role AKT plays in supporting metabolism in proliferating lymphocytes.[30] Activation of ERK in response to TCR stimulation is largely, but not entirely, dependent on ZAP70.[31] We examined the activation of TCR through evaluation of phosphorylation of ZAP70 and its downstream factors such as AKT. Consequently, we observed a reduction in activating phosphorylation of all members including ZAP70 and AKT, confirming that vorinostat inhibits TCR signaling by both down-regulation of the expression of several members of the pathway as well as by phosphorylation of key tyrosine kinases.

Given the broad activity of vorinostat, the inhibition of other kinases affecting T-cell function cannot be excluded. The increase of the SRC family tyrosine kinase FYN, also observed by Peart *et al.*,[32] seems to play an important role in the fine-tuning of TCR signaling. As previously described by Filby *et al.*,[33] FYN phosphorylates several negative regulators of T-cell signaling, suggesting its involvement in terminating TCR signals. On the other hand, another SRC family tyrosine kinase, LCK, is a key initiator of TCR signal transduction and leads to recruitment and activation of ZAP70.[34] Therefore, up-regulation of FYN, correlated with modest (1.5 to 2-fold) down-regulation of LCK and significant decreases in the expression of other important TCR signaling molecules (LAT) following vorinostat treatment, is sufficient to confer inhibition of TCR signaling. This inhibition is reflected in low phosphorylation levels of the central factor of TCR signaling – ZAP70.

In this study, Connectivity Maps were used to identify other molecules that could potentially be used in combination for treatment of patients resistant to PUVA with or without interferon-α. The molecules with the highest scores included the HDAC inhibitors vorinostat and Scriptaid,[35] as well as tanespimycin (17-AAG) and geldanamycin, known anticancer antibiotics that bind HSP90 and have antitumor activity in both leukemias[36] and solid cancers.[37] Furthermore, H-7, a PKC inhibitor, has been found to inhibit tumor cell invasion and metastasis in melanoma cells via suppression of phosphorylated ERK1/2.[38] Additionally, CTCL-derived tumor cells of Th2 phenotype have been shown to be resistant to interferon-α and interferon-γ.[39] In this light, molecules identified by Connectivity Map may result in more efficient treatment of CTCL.

Clinical trials of vorinostat, alone or in combination therapy, are on-going and are showing the drug's promising anti-cancer activities in both hematologic and solid tumors. The molecular events underlying the synergistic effect obtained from using vorinostat in combination remain to be fully elucidated; plausibly, it will be found that the mechanisms are dependent on the tumor cell type, specific molecular events and the precise agent added. So far there are only a limited number of reports that have focused on describing the interactions between HDAC inhibitors (including vorinostat) and inhibitors targeting PI3K and all have centered on LY294002.[40] Our current work indicates that a more potent and selective, hence less toxic, inhibitor of PI3K – ETP-45658 – has comparable synergy to LY294002 with vorinostat. Several properties that are critical for therapeutic agents differentiate ETP-45658 from previously tested PI3K inhibitors, including wortmannin and LY294002;[41] the main property is that ETP-45658 is highly selective for class IA PI3K.[22] ETP-45658 is, therefore, an attractive candidate for further clinical studies in combination with vorinostat and other HDAC inhibitors. For the combination of vorinostat and 17-AAG, we observed the opposite effect to that described in human leukemia cells[42] and mantle cell lymphoma.[43] Our data showed that co-administration of vorinostat and 17-AAG resulted in an antagonistic interaction, which could be related to the fact that vorinostat by itself already inhibits expression of HSP90. This result suggests that co-administration of vorinostat and 17-AAG should be avoided in CTCL. Moreover, we observed a correlation between the levels of expression of the targets of the inhibitors used following vorinostat treatment and the effect of the combination. Whenever the molecule targeted by the inhibitor was up-regulated (GSK-3β, PIM), the combination therapy resulted in synergistic or additive interactions. Furthermore, down-regulation of HSP90 (a target of 17-AAG) following vorinostat treatment showed an antagonistic effect of coadministration of 17-AAG with vorinostat. This suggests that inhibitors of genes whose levels increase significantly following vorinostat treatment could be the potential candidates for successful combination therapy.

Our data provide substantial new information improving our knowledge and understanding of the action of vorinostat, and suggest that clinical trials of vorinostat, either alone or in combination, performed in CTCL should evaluate the drug's *in vivo* effect on the signal transduction of TCR and correlate the results with the treatment response. In addition, our study has several clinical implications. First, PI3K inhibitors, such as ETP-45658, could be used in combination with vorinostat-based therapies; based on our current study, it is anticipated that the combination could be highly effective. Combining vorinostat with PI3K inhibitors is a rational approach to increase cytotoxic effects in CTCL. These results provide proof-of-principle that a comprehensive understanding of the mechanisms of action of vorinostat is central to designing rational combination approaches using HDAC inhibitors.

Authorship and Disclosures

Contribution: MBW designed the work, performed experiments, analyzed and interpreted the data, and wrote the manuscript; RV designed research, and interpreted the data; PdC and MER performed experiments; BH and DMP interpreted the data; JRB, CBA, JFML, MIL, and MH contributed vital reagents; MAP designed research, interpreted the data, and revised the manuscript; PLOR designed and research, revised the manuscript. No potential conflicts of interests relevant to this article were reported.

References

1. Girardi M, Heald PW, Wilson LD. The pathogenesis of mycosis fungoides. N Engl J Med. 2004:350(19):1978-88.
2. Wozniak MB, Tracey L, Ortiz-Romero PL, Montes S, Alvarez M, Fraga J, et al. Psoralen plus ultraviolet A +/- interferon-alpha treatment resistance in mycosis fungoides: the role of tumour microenvironment, nuclear transcription factor-kappaB and T-cell receptor pathways. Br J Dermatol. 2009;160(1): 92-102.
3. Lamb J, Crawford ED, Peck D, Modell JW, Blat IC, Wrobel MJ, et al. The Connectivity Map: using gene-expression signatures to connect small molecules, genes, and disease. Science. 2006(5795);313:1929-35.
4. Kelly H, Goldberg RM. Systemic therapy for metastatic colorectal cancer: current options, current evidence. J Clin Oncol. 2005;23(20): 4553-60.
5. O'Connor OA. Targeting histones and proteasomes: new strategies for the treatment of lymphoma. J Clin Oncol. 2005;23(26): 6429-36.
6. Marks PA, Jiang X. Histone deacetylase inhibitors in programmed cell death and cancer therapy. Cell Cycle. 2005;4(4):549-51.
7. Mitsiades CS, Mitsiades NS, McMullan CJ, Poulaki V, Shringarpure R, Hideshima T, et al. Transcriptional signature of histone deacetylase inhibition in multiple myeloma: biological and clinical implications. Proc Natl Acad Sci USA. 2004;101(2):540-5.
8. Richon VM, Sandhoff TW, Rifkind RA, Marks PA. Histone deacetylase inhibitor selectively induces p21WAF1 expression and gene-associated histone acetylation. Proc Natl Acad Sci USA. 2000;97(18):10014-9.
9. Gui CY, Ngo L, Xu WS, Richon VM, Marks PA. Histone deacetylase (HDAC) inhibitor activation of p21WAF1 involves changes in promoter-associated proteins, including HDAC1. Proc Natl Acad Sci USA. 2004; 101(5):1241-6.
10. Butler LM, Zhou X, Xu WS, Scher HI, Rifkind RA, Marks PA, Richon VM. The histone deacetylase inhibitor SAHA arrests cancer cell growth, up-regulates thioredoxin-binding protein-2, and down-regulates thioredoxin. Proc Natl Acad Sci USA. 2002; 99(18):11700-5.
11. Duvic M, Talpur R, Ni X, Zhang C, Hazarika P, Kelly C, et al. Phase 2 trial of oral vorinostat (suberoylanilide hydroxamic acid, SAHA) for refractory cutaneous T-cell lymphoma (CTCL). Blood. 2007;109(1):31-9.
12. Johnstone RW, Licht JD. Histone deacetylase inhibitors in cancer therapy: is transcription the primary target? Cancer Cell. 2003;4(1): 13-8.
13. Weiss A, Littman DR. Signal transduction by lymphocyte antigen receptors. Cell. 1994; 76(2):263-74.
14. Asadullah K, Friedrich M, Döcke WD, Jahn S, Volk HD, Sterry W. Enhanced expression of T-cell activation and natural killer cell antigens indicates systemic anti-tumor response in early primary cutaneous T-cell lymphoma. J Invest Dermatol. 1997;108(5): 743-7.
15. Querfeld C, Rosen ST, Guitart J, Kuzel TM. The spectrum of cutaneous T-cell lymphomas: new insights into biology and therapy. Curr Opin Hematol. 2005;12(4):273-8.
16. Ernst J, Nau GJ, Bar-Joseph Z. Clustering short time series gene expression data. Bioinformatics. 2005;21 (Suppl 1):i159-68.
17. Al-Shahrour F, Diaz-Uriarte R, Dopazo J. FatiGO: a web tool for finding significant associations of Gene Ontology terms with groups of genes. Bioinformatics. 2004;20(4): 578-80.
18. Ruefli AA, Ausserlechner MJ, Bernhard D, Sutton VR, Tainton KM, Kofler R, et al. The histone deacetylase inhibitor and chemotherapeutic agent suberoylanilide hydroxamic acid (SAHA) induces a cell-death pathway characterized by cleavage of Bid and production of reactive oxygen species. Proc Natl Acad Sci USA. 2001; 98(19):10833-8.
19. Zhang C, Richon V, Ni X, Talpur R, Duvic M. Selective induction of apoptosis by histone deacetylase inhibitor SAHA in cutaneous T-cell lymphoma cells: relevance to mechanism of therapeutic action. J Invest Dermatol. 2005;125(5):1045-52.
20. Watts JD, Affolter M, Krebs DL, Wange RL, Samelson LE, Aebersold R. Identification by electrospray ionization mass spectrometry of the sites of tyrosine phosphorylation induced in activated Jurkat T cells on the protein tyrosine kinase ZAP-70. J Biol Chem. 1994;269(47):29520-9.
21. Bauer B, Baier G. Protein kinase C and AKT/protein kinase B in CD4+ T-lymphocytes: new partners in TCR/CD28 signal integration. Mol Immunol. 2002;38(15): 1087-99.
22. Link W, Oyarzabal J, Serelde BG, Albarran MI, Rabal O, Cebriá A, et al. Chemical interrogation of FOXO3a nuclear translocation identifies potent and selective inhibitors of phosphoinositide 3-kinases. J Biol Chem. 2009;284(41):28392-400.
23. Marks P, Rifkind RA, Richon VM, Breslow R, Miller T, Kelly WK. Histone deacetylases and cancer: causes and therapies. Nat Rev Cancer. 2001;1(3):194-202.
24. Zhang CL, Kamarashev J, Qin JZ, Burg G, Dummer R, Döbbeling U. Expression of apoptosis regulators in cutaneous T-cell lymphoma (CTCL) cells. J Pathol. 2003;200(2): 249-54.
25. Rosato RR, Almenara JA, Dai Y, Grant S. Simultaneous activation of the intrinsic and extrinsic pathways by histone deacetylase (HDAC) inhibitors and tumor necrosis factor-related apoptosis-inducing ligand (TRAIL) synergistically induces mitochondrial damage and apoptosis in human leukemia cells. Mol Cancer Ther. 2003;2(12): 1273-84.
26. Gillenwater AM, Zhong M, Lotan R. Histone deacetylase inhibitor suberoylanilide hydroxamic acid induces apoptosis through both mitochondrial and Fas (Cd95) signaling in head and neck squamous carcinoma cells. Mol Cancer Ther. 2007;6(11): 2967-75.
27. Fantin VR, Loboda A, Paweletz CP, Hendrickson RC, Pierce JW, Roth JA, et al. Constitutive activation of signal transducers and activators of transcription predicts vorinostat resistance in cutaneous T-cell lymphoma. Cancer Res. 2008;68(10):3785-94.
28. Iwashima M, Irving BA, van Oers NS, Chan AC, Weiss A. Sequential interactions of the TCR with two distinct cytoplasmic tyrosine kinases. Science. 1994;263(5150):1136-9.
29. Janeway CA Jr, Bottomly K. Signals and signs for lymphocyte responses. Cell. 1994; 76(2):275-85.
30. Juntilla MM, Koretzky GA. Critical roles of the PI3K/Akt signaling pathway in T cell development. Immunol Lett. 2008;116(2): 104-10.
31. Griffith CE, Zhang W, Wange RL. ZAP-70-dependent and -independent activation of Erk in Jurkat T cells. Differences in signaling induced by H2o2 and Cd3 cross-linking. J Biol Chem. 1998;273(17):10771-6.
32. Peart MJ, Smyth GK, van Laar RK, Bowtell DD, Richon VM, Marks PA, et al. Identification and functional significance of genes regulated by structurally different histone deacetylase inhibitors. Proc Natl Acad Sci USA. 2005;102(10):3697-702.
33. Filby A, Seddon B, Kleczkowska J, Salmond R, Tomlinson P, Smida M. Fyn regulates the duration of TCR engagement needed for commitment to effector function. J Immunol. 2007;179(7):4635-44.
34. Straus DB, Weiss A. Genetic evidence for the involvement of the lck tyrosine kinase in signal transduction through the T cell antigen receptor. Cell. 1992;70:585-93.
35. Takai N, Ueda T, Nishida M, Nasu K, Narahara H. A novel histone deacetylase inhibitor, Scriptaid, induces growth inhibition, cell cycle arrest and apoptosis in human endometrial cancer and ovarian cancer cells. Int J Mol Med. 2006;17(2): 323-9.
36. Meyer PN, Roychowdhury S, Kini AR, Alkan S. HSP90 inhibitor 17AAG causes apoptosis in ATRA-resistant acute promyelocytic leukemia cells. Leuk Res. 2008;32(1): 143-9.
37. Zsebik B, Citri A, Isola J, Yarden Y, Szöllosi J, Vereb G. Hsp90 inhibitor 17-AAG reduces ErbB2 levels and inhibits proliferation of the trastuzumab resistant breast tumor cell line JIMT-1. Immunol Lett. 2006;104(1-2):146-55.
38. Tsubaki M, Matsuoka H, Yamamoto C, Kato C, Ogaki M, Satou T, et al. The protein kinase C inhibitor, H7, inhibits tumor cell invasion and metastasis in mouse melanoma via suppression of ERK1/2. Clin Exp Metastasis. 2007;24(6):431-8.
39. Dummer R, Döbbeling U, Geertsen R, Willers J, Burg G, Pavlovic J. Interferon resistance of cutaneous T-cell lymphoma-derived clonal T-helper 2 cells allows selective viral replication. Blood. 2001;97(2):523-7.
40. Rahmani M, Yu C, Reese E, Ahmed W, Hirsch K, Dent P, Grant S. Inhibition of PI-3 kinase sensitizes human leukemic cells to histone deacetylase inhibitor-mediated apoptosis through p44/42 MAP kinase inactivation and abrogation of p21(CIP1/WAF1) induction rather than AKT inhibition. Oncogene. 2003;22(40):6231-42.
41. Hennessy BT, Smith DL, Ram PT, Lu Y, Mills GB. Exploiting the PI3K/AKT pathway for cancer drug discovery. Nat Rev Drug Discov. 2005;4(12):988-1004.
42. Rahmani M, Yu C, Dai Y, Reese E, Ahmed W, Dent P, Grant S. Coadministration of the heat shock protein 90 antagonist 17-allylamino- 17-demethoxygeldanamycin with suberoylanilide hydroxamic acid or sodium butyrate synergistically induces apoptosis in human leukemia cells. Cancer Res. 2003; 63(23):8420-7.
43. Rao R, Lee P, Fiskus W, Yang Y, Joshi R, Wang Y, et al. Co-treatment with heat shock protein 90 inhibitor 17-dimethylaminoethylamino-17-demethoxygeldanamycin (DMAG) and vorinostat: a highly active combination against human mantle cell lymphoma (MCL) cells. Cancer Biol Ther. 2009; 8(13): 1273-80.